

Surface and bulk contributions to the second-order nonlinear optical response of a gold filmFu Xiang Wang,¹ Francisco J. Rodríguez,¹ Willem M. Albers,² Risto Ahorinta,³ J. E. Sipe,⁴ and Martti Kauranen^{1,*}¹*Department of Physics, Tampere University of Technology, P.O. Box 692, FI-33101 Tampere, Finland*²*VTT Microtechnology and Sensors, P.O. Box 1300, FI-33101 Tampere, Finland*³*Optoelectronics Research Centre, Tampere University of Technology, P.O. Box 692, FI-33101 Tampere, Finland*⁴*Department of Physics and Institute for Optical Sciences, University of Toronto, Toronto, Ontario, Canada M5S 1A7*

(Received 9 July 2009; published 8 December 2009)

We use two-beam second-harmonic generation to separate the surface (electric dipole origin) and bulk (magnetic dipole and electric quadrupole origin) contributions to the second-order nonlinear optical response of an isotropic gold film. The bulk response is unambiguously observed and explained by momentum damping of electrons in a free-electron model. Although bulk effects could be enhanced by inhomogeneous local fields in metal nanostructures and have been used to model second-harmonic generation from metamaterials [Y. Zeng *et al.*, Phys. Rev. B **79**, 235109 (2009)], we find that surface effects dominate the nonlinearity. Our quantitative results for the surface and bulk parameters set the baseline for future descriptions of the second-order response of nanostructured metals.

DOI: [10.1103/PhysRevB.80.233402](https://doi.org/10.1103/PhysRevB.80.233402)

PACS number(s): 78.68.+m, 42.65.Ky, 68.47.De, 78.66.Bz

Second-order nonlinear optical processes, such as second-harmonic generation (SHG), are forbidden in centrosymmetric materials on the electric dipole level of the light-matter interaction.¹ Symmetry is broken at material interfaces, thus giving rise to a dipolar surface nonlinearity.² Multipole (magnetic dipole and electric quadrupole) interactions, however, allow second-order effects even in centrosymmetric bulk materials.² Separation between the surface and bulk effects has been a long-standing problem in nonlinear optics for a number of reasons. For example, the contribution to the SHG signal of one of the important bulk parameters (usually denoted as γ) cannot be separated from surface contributions.³ In addition, another bulk parameter (usually denoted as δ') makes no contribution in traditional measurement techniques.^{2,4,5} The recently developed two-beam SHG technique,^{6,7} however, allows for an unambiguous and quantitative determination of this parameter independent of any surface contribution, as already shown for dielectric samples.^{6,8,9} Hence, we refer to it as the “separable” bulk parameter. Roughly speaking, its contribution to the SHG signal can be expected to become more important when the field inside the metal contains a large number of plane-wave expansion coefficients.

Thus, the separation between the surface and bulk effects becomes particularly important to describe the nonlinear response of metal nanostructures and metamaterials. The local-field distribution in such structures is highly inhomogeneous including several plane-wave components, which could enhance coupling to bulk effects. Indeed, SHG from split-ring resonators has recently been described by bulk effects.^{10–12} On the other hand, surface effects are usually thought to be important in the second-order response of metals^{13–16} and have been implied for the case of plasmonic nanoparticles^{17,18} and nanodimers.¹⁹

Bulk effects are naturally included in the free-electron theories of metals.^{3,20,21} Traditional versions of these theories, however, imply that the separable bulk contribution vanishes.³ Proper theoretical treatment of surface mechanisms, on the other hand, is very difficult.^{3,13–15,21–26} Because of the conflicting interpretations of recent experiments and open theoretical questions, it is evident that experiments on

simple model systems are needed to improve the understanding of the nonlinear response of metals.

In this Brief Report, we separate the surface and bulk contributions to SHG from a flat gold film. The separable bulk contribution, which vanishes in traditional free-electron models,^{3,20,21} is unambiguously observed and explained by the momentum relaxation of electrons. Nevertheless, the nonlinear signals are dominated by surfacelike effects, which should thus not be neglected in future theoretical approaches to describe the nonlinear response of nanostructures and metamaterials. Our quantitative results for the nonlinear surface and bulk parameters set the baseline for such theoretical work.

At frequencies away from any interband transitions, noble metals can often be treated as an isotropic free-electron gas. The SH response of a flat surface of any isotropic material is

$$P_i^{surface}(2\omega) = \chi_{ijk} e_j(\omega) e_k(\omega), \quad (1)$$

where $P_i^{surface}(2\omega)$ and $e_{j,k}(\omega)$ are the Cartesian components of the SH surface polarization and the electric field at the fundamental frequency, respectively, and χ_{ijk} are the components of the electric dipole allowed second-order surface susceptibility tensor. For isotropic and centrosymmetric materials, the nonvanishing tensor components are χ_{zzz} , $\chi_{zxz} = \chi_{zyy}$, and $\chi_{xxz} = \chi_{xzx} = \chi_{yyz} = \chi_{yzy}$, where z is the surface normal [Fig. 1(a)].

Proper use of Eq. (1) requires great care because the surface susceptibility can be defined equally well in terms of the fundamental field and nonlinear polarization sheet inside or outside the nonlinear material. For vacuum-material interfaces, the most natural choice is to evaluate the fundamental field just inside and place the polarization sheet just outside,^{3,21} defining the conventional (C) surface tensor χ_{ijk}^C . For more practical purposes, however, it may be convenient to refer all quantities to their internal (I) or external (E) values, leading to surface tensors χ_{ijk}^I and χ_{ijk}^E , respectively. We will pay particular attention to the various definitions of the surface parameters, which has given rise to considerable confusion over the years.

The effective SH source polarization of isotropic and cen-

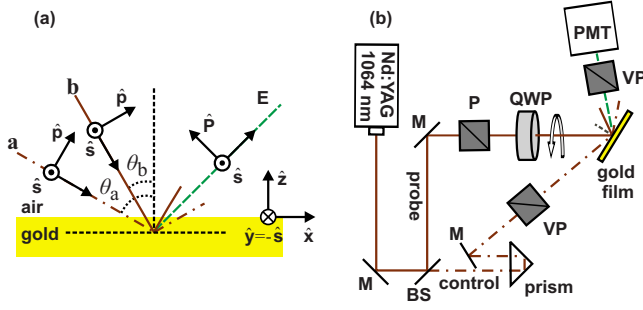


FIG. 1. (Color online) Two-beam second-harmonic generation. (a) Surface geometry where two fundamental beams **a** and **b** intersect at a gold film and the second-harmonic signal **E** generated jointly by the two beams is detected in reflection. (b) Experimental setup: BS, beam splitter; M, mirror; P, polarizer; QWP, zero-order quarter-wave plate; VP, variable-angle polarizer; and PMT, photomultiplier tube. A prism in the path of the control beam adjusts its delay and synchronizes the pulse with that of the probe beam.

troisymmetric bulk materials, on the other hand, is of the form²⁰

$$\mathbf{P}^{bulk}(2\omega) = \beta \mathbf{e}(\omega) [\nabla \cdot \mathbf{e}(\omega)] + \gamma \nabla [\mathbf{e}(\omega) \cdot \mathbf{e}(\omega)] + \delta' [\mathbf{e}(\omega) \cdot \nabla] \mathbf{e}(\omega), \quad (2)$$

where $\mathbf{e}(\omega)$ is the vectorial fundamental field and β , γ , and δ' are material parameters due to magnetic dipole and electric quadrupole effects. As this equation describes bulk effects, fields inside the material must be used. This suggests that a quantitative comparison between the surface and bulk parameters is facilitated by using the tensor χ_{ijk}^j for the surface response.

For homogeneous and isotropic materials, the first term of Eq. (2) can be neglected since $\nabla \cdot \mathbf{E} = \epsilon^{-1} \nabla \cdot \mathbf{D}$ vanishes. The second term leads to the surfacelike contribution to the measured signals. This contribution can be taken into account^{27,28} by defining the effective surface components as $\chi_{zzz}^{C,eff} = \chi_{zzz}^C + \gamma / \epsilon(2\omega)$, $\chi_{zxx}^{C,eff} = \chi_{zxx}^C + \gamma / \epsilon(2\omega)$, and $\chi_{xxz}^{C,eff} = \chi_{xxz}^C$, where the bulk parameter γ has been rescaled by the dielectric constant of the material at the second-harmonic frequency $\epsilon(2\omega)$ in order to conform with the conventional surface response.^{3,21} Finally, the third term δ' is the one separable from the surface response and can be directly addressed only by SHG using two noncollinear fundamental beams.^{6–8}

The origin of the metal nonlinearity has been widely discussed since the early days of nonlinear optics. The original free-electron-gas model²⁰ had limitations in describing electron dynamics near the surface,²¹ until the hydrodynamic model provided a more detailed analysis to estimate the nonlinear surface and bulk currents.³ The bulk nonlinearity arises from the Lorentz and convective forces; nevertheless, the separable bulk parameter δ' was predicted to vanish.^{3,20,21} Furthermore, these models predict that the surface component χ_{zxx}^C vanishes and hence the effective surface component $\chi_{zxx}^{C,eff} = \gamma / \epsilon(2\omega)$ actually arises from the bulk. The surface component χ_{zzz}^C , on the other hand, can depend sensitively on the surface details and exhibit resonances.^{24–26}

Most early SHG experiments on metals were restricted to

the determination of the effective surface components and comparing them to theoretical models.^{3,13,22–26} Nevertheless, the issue is still under active investigation, with widely varying results.^{15,16} The bulk effects have received much less attention, but have recently been used to model SHG from metal nanostructures.^{10–12} Bulk effects were also discussed in a study of a composite structure of alternating metallic and dielectric layers, but there were problems in separating them from surface effects.²⁹ Nevertheless, the separable bulk parameter δ' has not been unambiguously identified before.

To access the separable bulk contribution δ' , we use two-beam SHG [Fig. 1(a)]. Two plane waves (control **a** and probe **b**) at the fundamental frequency ω are applied on the sample in the same plane of incidence (xz plane) but at different angles of incidence and the SH signal at 2ω generated jointly by the fundamental beams is detected in reflection. We take the positive z axis as the surface normal and pointing into air. The unit vector $\hat{\mathbf{p}}$ is in the plane of incidence and depends on the propagation direction of each beam while $\hat{\mathbf{s}}$ is perpendicular to the plane of incidence and is the same for all beams.

Because of isotropy, the SH field components have the following dependence on the fundamental fields:⁸

$$E_p^{total} = f_{ppp} a_p b_p + f_{pss} a_s b_s, \quad (3)$$

$$E_s^{total} = f_{sps} a_p b_s + f_{ssp} a_s b_p, \quad (4)$$

where the expansion coefficients f_{ijk} depend linearly on the susceptibility components and are defined with respect to the fundamental (a and b) and SH (E) fields evaluated in air above the sample. The coefficients also depend on the Fresnel factors between air and gold, and on the (lossy) propagation inside the gold. All these effects are fully accounted for by the Green's function formalism of nonlinear optics.³⁰ The expansion coefficients can be measured by using different combinations of the polarizations of the fundamental and SH beams. After that, the surface and bulk susceptibility components can be extracted from the experimental results using the theoretical formalism.

Our method allows even more direct evidence to be obtained on δ' . Due to isotropy, the s -polarized SH signals from the effective surface and separable bulk contributions are⁶

$$E_s^{surface} \propto \chi_{xxz}^{C,eff} \left(a_p b_s + \frac{\sin \theta_b}{\sin \theta_a} a_s b_p \right), \quad (5)$$

$$E_s^{bulk} \propto i \delta' (a_p b_s - a_s b_p), \quad (6)$$

where θ_a and θ_b are the angles of incidence of the fundamental beams. When θ_a and θ_b have the same sign, the surface and bulk effects have a very different dependence on the polarizations of the fundamental beams.

Our experiments [Fig. 1(b)] are thus based on detailed polarization measurements of the SH response. A pulsed Nd:YAG laser (wavelength 1064 nm, pulse length 60 ps, pulse energy 0.15 mJ, and pulse repetition rate 1000 Hz) is the source of fundamental light. The laser output is collimated to a spot size of $\sim 400 \mu\text{m}$ and split into two beams

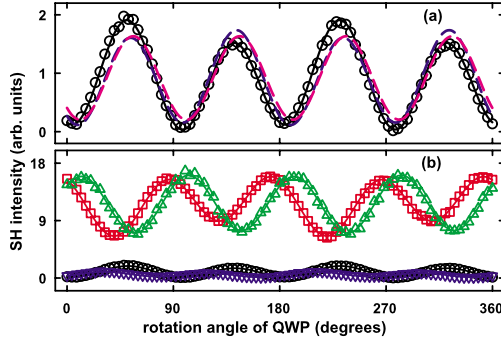


FIG. 2. (Color online) The second-harmonic intensity as a function of the rotation angle of QWP. (a) $(-45^\circ, s)$ signal fitted to surface-only models (dashed lines) based on external and internal fields and a model with both surface and bulk contributions (black solid line). (b) The black dots, red squares, green up-pointing triangles, and blue down-pointing triangles are the data for $(-45^\circ, s)$, $(-45^\circ, p)$, $(p, -45^\circ)$, and $(s, -45^\circ)$, respectively. The lines correspond to a simultaneous fit of all data to a model with both surface and bulk contributions.

of nearly the same intensity, which intersect at the gold film with incident angles of 16.4° (probe beam) and 43.8° (control beam) and the same plane of incidence. The control beam is linearly polarized with a variable-angle calcite Glan polarizer (extinction ratio $\sim 4 \times 10^{-6}$) and its polarization is kept fixed during each measurement. The probe beam is first p polarized and then a zero-order quarter-wave plate (QWP) continuously modulates its polarization while linearly polarized SH signals are recorded in reflection with a photomultiplier tube. Different combinations of the control and SH polarization are used to fully determine the nonlinear response of the sample.

TABLE I. Nonlinear susceptibility components of gold and their relative contributions to the measured polarization-dependent SH signals. Several measurements using different samples yielded results within 30% of the shown ones. For completeness, we include the results for the effective surface components following the conventional definition where the fundamental fields are evaluated in the metal and the source polarization is placed outside (tensor $\chi_{ijk}^{C,eff}$, column 2) and the alternative choices where the components are referenced to internal (tensor $\chi_{ijk}^{I,eff}$, column 3) or external (tensor $\chi_{ijk}^{E,eff}$, column 4) quantities. Note that the pure bulk parameter δ' can only be defined in terms of the internal fields and should be compared to surface parameter defined in the same way (column 3). The absolute values were calibrated against a 10-mm-thick X-cut quartz crystal. The nonlinear response of quartz is dominated by the χ_{xxx} component of the second-order susceptibility tensor. However, the literature values of this component vary between 0.6 and 0.8 pm/V (Refs. 1, 15, and 16) which is a remaining uncertainty in our results.

Relative magnitudes of susceptibility tensor components (for absolute magnitudes multiply by 7.8×10^{-14} cm ² /statvolt)				Contribution to the measured SH signals				Character
	Conventional	Internal fields	External fields	f_{ppp}	f_{pss}	f_{sps}	f_{sss}	
Expression	$\chi_{zzz}^{C,eff} = \chi_{zzz}^C + \frac{\gamma}{\epsilon(2\omega)}$	$\chi_{zzz}^{I,eff} = \chi_{zzz}^{C,eff} \epsilon(2\omega)$	$\chi_{zzz}^{E,eff} = \frac{\chi_{zzz}^{C,eff}}{\epsilon^2(\omega)}$	1.3				Surface and bulk
Value	47.6	250	0.017					
Expression	$\chi_{zxx}^{C,eff} = \chi_{zxx}^C + \frac{\gamma}{\epsilon(2\omega)}$	$\chi_{zxx}^{I,eff} = \chi_{zxx}^{C,eff} \epsilon(2\omega)$	$\chi_{zxx}^{E,eff} = \chi_{zxx}^{C,eff}$	1.5	1.0			Surface and bulk
Value	0.19	1	0.19					
Expression	$\chi_{xxz}^{C,eff} = \chi_{xxz}^C$	$\chi_{xxz}^{I,eff} = \chi_{xxz}^{C,eff}$	$\chi_{xxz}^{E,eff} = \frac{\chi_{xxz}^{C,eff}}{\epsilon(\omega)}$	3.5		2.2	0.6	Surface only
Value	3.6	3.6	0.068					
Expression		δ'		0.004		0.2	0.1	Bulk only
Value		2.7						

Our metal sample, made by sputtering, consisted of a standard microscope glass substrate, a 10-nm-thick adhesion layer of indium oxide, and a 150-nm-thick gold film. The exact thickness of gold is not important because no appreciable light reaches the gold-substrate interface. The film is isotropic in the plane of the substrate as verified by measurements at different azimuthal orientations. The complex refractive indices of the gold film, measured with a spectroscopic ellipsometer, are $n(\omega) = 0.21 + i7.26$ and $n(2\omega) = 0.45 + i2.25$.

To obtain direct evidence of δ' , we first measured the SH signal for the fixed polarizations $(-45^\circ, s)$, where the first label indicates the polarization of the control beam and the second that of the SH beam. The data [Fig. 2(a)] can be properly fitted only by using a model based on interference between the surface and bulk contributions [Eqs. (5) and (6)].

To determine the expansion coefficients f_{ijk} , we measured the SH signals for the polarization combinations $(-45^\circ, s)$, $(-45^\circ, p)$, $(p, -45^\circ)$, and $(s, -45^\circ)$. The data and their simultaneous fits to the theoretical model [Fig. 2(b)] yielded the relative values of the nonlinear components $\chi_{ijk}^{C,eff}$ and δ' . Finally, we calibrated their absolute values against a quartz crystal by adapting our earlier calibration method⁹ for reflection.

The magnitudes of the susceptibility components are shown in Table I. Comparison between the bulk parameter δ' and the components of the surface susceptibility $\chi_{ijk}^{I,eff}$ quoted in terms of the internal fields (column 3 of Table I) suggests that the response is dominated by the surface component $\chi_{zzz}^{I,eff}$, where the bulk parameter γ makes only a minor contribution. Nevertheless, the separable bulk component δ' is unambiguously detected, although traditional models predict that this component should vanish.

To understand the nonvanishing δ' component, we extended the free-electron hydrodynamic model to include the momentum relaxation of electrons, which arises from electron collisions with the metal lattice. This yields new predictions for γ and δ' (Ref. 31),

$$\gamma = \chi(\Omega) \frac{\chi(\omega)}{2en_0}, \quad (7)$$

$$\delta' = -\chi(\Omega) \left[\frac{\chi(\omega)}{en_0} + \frac{m\omega^2\chi^2(\omega)}{e^3n_0^2} \right], \quad (8)$$

where $-e$ is the electron charge, m the electron mass, and n_0 the electron number density. The linear susceptibilities at frequencies ω and $\Omega=2\omega$ are $\chi(\omega)=-e^2n_0[m\omega(\omega+i/\tau)]^{-1}$ and $\chi(\Omega)=-e^2n_0[m\Omega(\Omega+i/\tau)]^{-1}$ with τ the relaxation time. The two terms in Eq. (8) arise from the Lorentz and convective forces, respectively. With no damping ($\tau \rightarrow \infty$), the sum is seen to vanish due to destructive interference between the two forces. With damping, however, such symmetry is broken and δ' is nonvanishing.

To improve the reliability of the predictions,³ the theoretical expressions were evaluated by replacing the dielectric constants of the free-electron theory by the measured ones. Under the assumption that χ_{xx}^C vanishes, the measured magnitude $|\gamma|$ was found to be larger by a factor 2.2 compared to theory. The agreement is very good, considering the uncertainties in the experimental calibration. However, the measured $|\delta'|$ is larger by a factor of 20 compared to theory. This difference arises from the fact that, being relaxation induced, δ' possesses an extreme sensitivity to the parameters of the model.

It is important to note that the values of the surface components depend strongly on whether they are referenced using the fields in the metal ($\chi_{ijk}^{L,eff}$, column 3 of Table I) or

outside ($\chi_{ijk}^{E,eff}$, column 4 of Table I).²⁷ The truly meaningful comparison between the components can therefore only be made by evaluating their contributions to the measured SH signals, which is independent of the choice of reference. This comparison (columns 5–8 of Table I) shows that the surface-like contributions dominate and that the pure bulk component δ' makes only a minor contribution. Note however, that $\chi_{zxx}^{C,eff}$, which is also believed to have bulk origin, makes an appreciable contribution.

We finally consider the implications of these results for metal nanostructures, including metamaterials. The local fundamental field distribution in such structures is highly inhomogeneous containing several plane-wave components, which could enhance the signal from the δ' parameter and the bulk effects. However, theoretical models based on bulk effects are able to account only for the parameters γ and δ' . Although γ makes an appreciable contribution to the measured SH signals, surface components χ_{zzz}^C and χ_{xxz}^C are also important. On the other hand, γ can be accounted for by the effective surface contributions $\chi_{zzz}^{C,eff}$ and $\chi_{zxx}^{C,eff}$. We therefore conclude that, on the simplest level, the second-order response of metals is better described by surface rather than bulk effects. Ideally, both surface and bulk effects should be taken into account. Our results thus set the baseline for future models of the second-order response of nanostructured metals by providing quantitative surface and bulk parameters that can be used to describe the local nonlinearity that interacts with the local fields.

We acknowledge the support by the Academy of Finland (Grants No. 107009, No. 108538, and No. 114913) and by the Nanophotonics Program of the Ministry of Education of Finland. We also acknowledge experimental help by I. Kettunen, discussions with S. Cattaneo, and M. Centini for sending Ref. 31 to us.

*Corresponding author; martti.kauranen@tut.fi

¹R. W. Boyd, *Nonlinear Optics* (Academic, San Diego, 1992).

²Y. R. Shen, *Appl. Phys. B: Lasers Opt.* **68**, 295 (1999).

³J. E. Sipe *et al.*, *Phys. Rev. B* **21**, 4389 (1980).

⁴X. Wei *et al.*, *J. Phys. Chem. B* **104**, 3349 (2000).

⁵H. Held *et al.*, *Phys. Rev. B* **66**, 205110 (2002).

⁶S. Cattaneo and M. Kauranen, *Phys. Rev. B* **72**, 033412 (2005).

⁷P. Figliozzi *et al.*, *Phys. Rev. Lett.* **94**, 047401 (2005).

⁸F. J. Rodríguez *et al.*, *Opt. Express* **15**, 8695 (2007).

⁹F. J. Rodríguez *et al.*, *Opt. Express* **16**, 8704 (2008).

¹⁰M. W. Klein *et al.*, *Science* **313**, 502 (2006).

¹¹N. Feth *et al.*, *Opt. Lett.* **33**, 1975 (2008).

¹²Y. Zeng *et al.*, *Phys. Rev. B* **79**, 235109 (2009).

¹³J. C. Quail and H. J. Simon, *Phys. Rev. B* **31**, 4900 (1985).

¹⁴R. Murphy *et al.*, *Phys. Rev. Lett.* **63**, 318 (1989).

¹⁵D. Krause *et al.*, *J. Appl. Phys.* **96**, 3626 (2004).

¹⁶K. A. O'Donnell and R. Torre, *New J. Phys.* **7**, 154 (2005).

¹⁷S. Kujala *et al.*, *Phys. Rev. Lett.* **98**, 167403 (2007).

¹⁸S. Kujala *et al.*, *Opt. Express* **16**, 17196 (2008).

¹⁹B. K. Canfield *et al.*, *Nano Lett.* **7**, 1251 (2007).

²⁰N. Bloembergen *et al.*, *Phys. Rev.* **174**, 813 (1968).

²¹J. Rudnick and E. A. Stern, *Phys. Rev. B* **4**, 4274 (1971).

²²M. Corvi and W. L. Schaich, *Phys. Rev. B* **33**, 3688 (1986).

²³A. Liebsch and W. L. Schaich, *Phys. Rev. B* **40**, 5401 (1989).

²⁴J. A. Maytorena *et al.*, *Phys. Rev. B* **51**, 2556 (1995).

²⁵B. S. Mendoza and W. L. Mochan, *Phys. Rev. B* **53**, 4999 (1996).

²⁶W. L. Schaich, *Phys. Rev. B* **61**, 10478 (2000).

²⁷V. Mizrahi and J. E. Sipe, *J. Opt. Soc. Am. B* **5**, 660 (1988).

²⁸J. E. Sipe *et al.*, *Phys. Rev. B* **35**, 9091 (1987).

²⁹M. C. Larciprete *et al.*, *Phys. Rev. A* **77**, 013809 (2008).

³⁰J. E. Sipe, *J. Opt. Soc. Am. B* **4**, 481 (1987).

³¹M. Centini *et al.*, *Proc. SPIE* **7354**, 73540F (2009).